TESLA - COLLABORATION

Wiggler Options for TESLA Damping Ring

R. Brinkmann, J. Pflüger, V. Shiltsev, N. Vinokurov*, P. Vobly*

DESY, *Budker INP, Novosibirsk

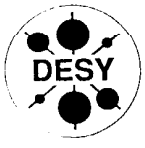

October 1995, TESLA 95-24

Wiggler Options for TESLA Damping Ring

R. Brinkmann, J. Pflüger, V. Shiltsev *
DESY, Notkestrasse 85, 22603, Hamburg, GERMANY
N. Vinokurov, P. Vobly
Budker Institute of Nuclear Physics, 630090 Novosibirsk, RUSSIA

October 30, 1995

Abstract

In this article we make a design study for damping wigglers for the TESLA Linear Collider damping ring. The parameter space for the wiggler design is estimated. Four designs based on permanent magnet technology are proposed and discussed.

1 Introduction

The TESLA linear collider design [1] intends to use damping ring(s) for great reduction of the beams phase space volumes before injection in the main linac. The positron beam is produced on a target with an expected normalized transverse emittance as large as 0.01 m [2] and a damping ring appears to be the only solution to squeeze the emittance within a linac cycle time of T_c=200 ms [3]. As an alternative, a RF gun can be used to achieve the design emittance of the electron beam [4], which in this case would allow to save one of two damping rings. Due to injection/ejection technological limitations the circumference of the ring should be comparably large and synchrotron radiation in bending magnets can not provide a sufficiently short damping time. Magnetic wigglers have been considered to be installed in the damping ring in order to enforce radiative emittance damping [6].

In this article we proceed further in the consideration of the wigglers for the TESLA damping ring. Section 2 is devoted to general consideration of the wiggler and main requirements on it are derived from the needs of the project. In Section 3 we consider four variants of permanent magnet wigglers. Finally, in Section 4 we briefly discuss advantages and disadvantages of the proposed options.

2 Wiggler for Radiative Damping

The TESLA damping ring design should provide a low-emittance beam which after the bunch length compressor goes to the main linac. Basic parameters of the ring are given in the Table 1.

*on leave from Budker Institute of Nuclear Physics, 630090 Novosibirsk, RUSSIA

Table 1: Basic Parameters of TESLA Damping Ring

Energy	E	3.3	GeV
Cycle time	T_c	200	ms
No. of bunches	N_b	~ 1100	
Particles/bunch	N_e	$3.6{\cdot}10^{10}$	
Bunch length	σ_s	~ 1	cm
Damping times	$\tau_s/\tau_{x,y}$	18.5/37	ms
Norm. emittances			
at injection	$\epsilon_x^0/\epsilon_y^0$	$10^4/10^4$	μm
at ejection	ϵ_x/ϵ_y	10/0.2	μm

The circumference of the ring is not specified in the Table 1, because at present time there are some approaches to solve injection/ejection issues that leads to spread of the required ring circumferences. The problem is that the TESLA design intends a bunch train duration of about 800 μs (or about 240 km length) in the main linac. The bunch train must be compressed in a storage ring and then expanded when extracted out of it. Thus, the injection and ejection of every bunch has to be done individually. If one assumes to use a kicker for the ejection with rise/fall time τ, then the circumference of the ring is about $C[km] \simeq \tau[\mu s]/3$. For example, the "dog-bone" proposal for the damping ring assumes ultimate conventional kickers with $\tau \sim 60$ ns, and therefore, $C \simeq 20$ km [5]. The "dog-bone" ring consists of two long (about 10 km) straight sections which share the tunnel of the main linac and a pair of arcs at the ends. The necessary wigglers are to be installed in the straight sections. Under assumption of using somewhat modified injection/ejection scheme with several deflecting elements [7, 8] the ring with circumference of about 6.3 km in the existing HERA tunnel was discussed in Ref.[9].

Presently, there are some novel schemes of the fast kicker (e.g. superfast *beam-beam kicker* [10]) under consideration which allow to get $\tau \simeq 7$ ns and less. Consequently, an option for a low-cost damping ring in the existing tunnel of the PETRA ring with $C \approx 2.3$ km must be taken into consideration.

In the following sections we consider damping wiggler designs for two extreme cases, namely, the "dog-bone" damping ring with a circumference of 20 km, and the 2.3 km long damping ring in the PETRA tunnel.

With the repetition frequency of the linac $1/T_c$ =5 Hz, the vertical damping time τ_y has to be about 5.5 times less than T_c because the vertical emittance must be damped to the design value:

$$\epsilon_y \simeq \epsilon_y^0 e^{-2T_c/\tau_y} \approx \frac{\epsilon_y^0}{50000}. \quad (1)$$

Here for simplicity we assume that there is no significant impact of residual vertical dispersion and coupling coefficient $\theta_c^2 = \epsilon_y/\epsilon_x$ is smaller than the design emittance ratio of 0.02. As the vertical damping time $\tau_y \approx 37$ ms is about two times of the longitudinal one $\tau_s = E/(U_0 f_0)$ ($E = 3.3$ GeV, f_0 is the revolution frequency) then one needs to provide the energy loss per turn U_0 of

$$U_0 = \frac{2E}{f_0 \tau_y} \simeq 0.6[MeV] \cdot C[km]. \quad (2)$$

that is about 12 MeV for the "dog-bone" option and about 1.4 MeV for the 2.3 km ring.

As the losses are due to synchrotron radiation in the magnetic field B then :

$$U_0 = \int P_\gamma dL, \quad P_\gamma[MeV/m] = 1.26 \cdot 10^{-3} E^2[GeV] B^2[T] \quad (3)$$

and therefore, for the TESLA DR the necessary damping integral must be equal to:

$$I_D = \int B^2 dL \, [T^2 m] = 43.4 \cdot C[km]. \quad (4)$$

that gives about 870 T^2m for the "dog-bone" and about 100 T^2m for the 2.3 km machine in the PETRA tunnel.

Quantum fluctuations of the synchrotron radiation lead to growth of the horizontal emittance (see, e.g. [11]):

$$\frac{1}{\gamma}\frac{d\epsilon_x}{dL} = C_Q E^5 \left\langle \frac{\mathcal{H}}{\rho^3} \right\rangle, \quad C_Q = 2.06 \cdot 10^{-11} \, m^2 GeV^{-5}, \quad (5)$$

here the brackets $< ... >$ mean average value of invariant $\mathcal{H} = (\eta^2 + (\beta_x \eta' - \beta_x' \eta/2)^2)/\beta_x$ (η is the dispersion function) over the bending radius ρ in a third power.

For the wiggler with period λ and piecewise constant field of B_0 (square wiggler) the radius is also piecewise constant ρ_0 and simple calculations give:

$$\left\langle \frac{\mathcal{H}}{\rho^3} \right\rangle \approx \frac{\beta_x \lambda^2}{48 \rho_0^5}, \quad (6)$$

where it was assumed that the mean beta function in the wiggler is much bigger than its period $\beta_x \gg \lambda$. For the wiggler with sinusoidal field $B_y(z) = B_w \cos(2\pi z/\lambda)$, one gets

$$\left\langle \frac{\mathcal{H}}{\rho^3} \right\rangle \approx \frac{\beta_x \lambda^2}{15\pi^3 \rho_w^5} \quad (7)$$

where ρ_w is the bending radius corresponding to the maximum field B_w.

The exact field shape can be influenced by the magnetic design of the wiggler. Wigglers with rectangular field distribution need to have the period λ much bigger than the wiggler's vertical gap g. Sinusoidal field shape can be obtained for any period length.

Taking into account that the major contribution takes place over the wiggler length $L < C$, the evolution of the horizontal emittance can be described by following equation:

$$\epsilon_x(t) \simeq (\epsilon_x^0 - \frac{c\tau_x}{2}\frac{d\epsilon_x}{dL}\cdot\frac{L}{C})e^{-2t/\tau_x} + \frac{c\tau_x}{2}\frac{d\epsilon_x}{dL}\cdot\frac{L}{C}. \quad (8)$$

The first term in (8) is about the vertical emittance because $\tau_x \approx \tau_y$, and, therefore, can be neglected if we want to establish the condition to get finally the design emittance ϵ_x:

$$\frac{d\epsilon_x}{dL}\cdot\frac{L}{C} < \frac{2\epsilon_x}{c\tau_x}. \quad (9)$$

Taking into account requirement (4) we obtain from (9)
for piecewise constant magnetic field wiggler:

$$\mathcal{J}_x\lambda^2 B_0^3 < 6\,T^3m^3. \quad (10)$$

and for the sinusoidal field wiggler with $\int B^2dL = B_w^2L/2$:

$$\mathcal{J}_x\lambda^2 B_w^3 < 29\,T^3m^3. \quad (11)$$

One can see that these circumference-independent requirements set limits on the wiggler period λ.

One more notation concerns a definite relation between magnetic field of the wiggler and the beam energy spread induced by synchrotron radiation (see, e.g. [11]):

$$\sigma_E^2 = \frac{<\Delta E^2>}{E^2} = C_E\gamma^2\frac{\left\langle\frac{1}{\rho^2}\right\rangle}{\left\langle\frac{1}{\rho^2}\right\rangle}, \quad C_E \approx 1.92\cdot 10^{-13}\,m. \quad (12)$$

As one assumes that the main contribution to the radiation damping comes from the wiggler with piecewise constant magnetic field B_0, the energy spread in the TESLA DR becomes equal to:

$$\sigma_E = \sqrt{\frac{C_E\gamma\epsilon B_0}{mc^2}} \approx 0.85\cdot 10^{-3}\sqrt{B_0[T]}. \quad (13)$$

For the sinusoidal magnetic field distribution σ_E is $\sqrt{8/3\pi} \approx 0.92$ times of the formula (13).

Thus, the longitudinal emittance of the DR bunches, $\sigma_s\cdot\sigma_E \propto \sigma_E^2$ is proportional to B_0, and as long as this parameter is important for the bunch length compression system, the peak wiggler magnetic field is limited. In this paper we consider the wiggler options with $B \leq 2\,T$, that corresponds to a quite acceptable value of $\sigma_E \leq 1.2\cdot 10^{-3}$.

Finally, one more aspect must be considered when choosing the optimum wiggler design concerning the total amount of chromaticity generated in the wiggler section. This chromaticity has to be compensated in the arcs and can be especially large for the "dog-bone" version of the damping ring.

If we assume a $FODO$ cell structure for the wiggler section L_w-meters long with betatron phase advance per cell equal to μ, the chromaticity is about

Table 2:

Parameter		"Dog-bone"	PETRA tunnel-DR
circumference	C	20 km	2.3 km
rev. frequency	f_0	15 kHz	130 kHz
bunch spacing in DR	τ_b	60 ns	7 ns
dc beam current	I_a	100 mA	860 mA
loss per turn	U_0	12 MeV	1.4 MeV
wiggler integral	$\int B^2 dL$	870 T^2m	100 T^2m
SR power loss	$U_0 \cdot I_a$	1.2 MW	
QF limit:			
piecewise field	$\beta_x \lambda^2 B_0^3$	$<$ 6 $T^3 m^3$	
sinusoidal field	$\beta_x \lambda^2 B_w^3$	$<$ 29 $T^3 m^3$	

$$\xi_{x,y} = \frac{\Delta\nu}{(\Delta p/p)} = -\frac{tg(\mu/2)}{\mu/2}\frac{L_w}{2\pi\beta_{x,y}}, \tag{14}$$

where again $\beta_{x,y}$ denotes mean beta function in the wiggler. Unfortunately, maximum acceptable value of the beta function is minimum of two figures: either the value of about 10 m to maintain beam instabilities within some limits as well as to provide smaller beam size in the vacuum chamber aperture (especially at injection), or by the emittance growth condition Eq.(10).

Thus, for the $FODO$ cell structure with $\mu = \pi/2$ one can estimate the chromaticity

$$\xi_{x,y} \simeq -0.02 \cdot L_w[m]. \tag{15}$$

In order to avoid excessive strength required for the sextupoles in the arcs, the chromaticity generated in the wiggler section must be kept within limits.

Table 2 summarizes the results of this Section. To find the optimum damping wiggler several conflicting requirements have to be taken into account:

- maximum magnetic field is desired to reduce the length of the wiggler,
- bigger peak field corresponds to larger longitudinal emittance of the damping ring,
- larger vertical gap increases instability limits,
- smaller wiggler period is favorable with respect to horizontal emittance generation in the wiggler,
- larger wiggler length reduces the necessary SR power absorption per unit length,
- smaller wiggler length allows to get smaller natural chromaticity of the wiggler section.

In the next section of this paper we assume a wiggler gap of 25 mm which allows for a vacuum aperture in the wiggler region of about 20 mm.

3 Wiggler Design Proposals

3.1 Permanent Magnet Technology

Today wigglers and undulators are widely used in both synchrotron radiation sources and Free Electron Lasers. During the last 15 years permanent magnet (PM) technology based initially SmCo and later on NdFeB material has been developed to build these devices [12, 13]. At intermediate field levels up to about 2T this technology is now almost exclusively used. Alternatives are superconducting (SC) wigglers which are used for high field applications up to about 10T and electromagnet (EM) wigglers which are only used in special cases. For comparable geometries the field levels of EM devices are normally well below those of PM systems.

The advantages of PM technology are evident: the devices are passive, which means they do not need any power supply, do not cause operational costs and require almost no maintenance. In dedicated synchrotron radiation sources numerous devices are routinely used. For example in DORIS III ten insertion devices build in PM technology with a total length exceeding 32m are routinely used.

For a damping wiggler the damping integral $I_D = \int B^2 dL$ is of central importance. In addition beam dynamics require the magnetic field to fill out a horizontal and vertical aperture characterized by the vertical gap g and a horizontal width w. The total magnetic energy needed to fill out this volume is given by:

$$\mathcal{E}_M \simeq \frac{gh}{2\mu_0} \int B^2 dL, \tag{16}$$

where $\mu_0 = 1.25 \cdot 10^{-6}\ V \cdot s/(A \cdot m)$.

Permanent magnet material is characterized by its $B-H$ demagnetization curve. The optimum operational point is chosen when the energy product $B \cdot H$ is maximum. In this case the volume of magnet material is minimized and given by :

$$V_m \simeq \frac{gh}{\mu_0 (BH)_{max}} \int B^2 dL, \tag{17}$$

The demagnetization curve of NdFeB is essentially a straight line throughout the second quadrant with a slope very close to 1. In this case

$$(B \cdot H)_{max} \simeq \frac{1}{2} B_r \frac{1}{2} H_c \approx \frac{B_r^2}{4\mu_0}, \tag{18}$$

where B_r is the remanent field, and H_c is the coercive force of the material. Depending on material quality the maximum energy product for NdFeB is in the range of typically 240 - 340 kJ/m^3. Assuming 300 kJ/m^3 the absolute lower limit of material for the PETRA DR is 0.33 m^3 and for the "dog-bone" DR 2.8 m^3. A cross section of $g \times w = 25 \times 50$ mm^2 is assumed in both cases. Leakage flux and stray fields generally lead to larger volumes. In the next three subsections three different approaches will be presented which have been optimized to have the point of operation close to the $(B \cdot H)_{max}$ value.

Table 3: Preliminary Design Parameters for the 0.5 T Square Wiggler

Parameter		Unit	Dog-Bone DR	PETRA DR
Damping integral	I_D	T^2m	870	100
Magnetic gap	g	mm	25	25
Width of magnet	w	mm	70	70
Height of magnet	h	mm	11	11
Period length	λ	mm	<2000	<2000
Peak field	B_0	T	0.5	0.5
Wiggler length	L	m	3480	400
Volume of material	V_m	m^3	5.36	0.62
Material per meter		kg/m	11.6	11.6

3.2 0.5 T Square Wiggler

A square wiggler produces a rectangular field distribution along the electron beam axis. This is in contrast to most wigglers which normally produce a sinusoidal field. The damping integral of a square wiggler having the same peak field and length is increased by a factor of two as compared to a sinusoidal one.

Fig .1 shows the cross section and flux line distribution perpendicular to the electron beam. Only one fourth of the structure is shown for numerical reasons. The beam position is at the origin at $X = Y = 0$. A pole piece with a trapezoidal cross section is to guide the magnetic flux generated by the permanent magnet. A soft iron flux return yoke avoids unnecessary stray flux. For a wiggler, of course, sections with alternating field directions are needed. The working point of the magnet is close to $(B \cdot H)_{max}$. The peak field as calculated with the MERMAID code [14] is 0.5 T.

The period length can be chosen quite arbitrarily over a wide range. Using eq. (10)

and assuming a mean horizontal beta function of 10 m, the period length can be as large as 2 m without violating the emittance condition. Table 3 shows a summary of preliminary design parameters for such a structure.

3.3 1.0 T Pure Permanent Magnet Wiggler

Pure permanent magnet wigglers where first proposed by Halbach [13]. They offer a simple way for a damping wiggler. Fig. 2 illustrates the magnetic setup. Pure permanent magnet devices can be treated with analytical formulae. The peak field is described by :

$$B_w = 1.8 B_r e^{-\pi g/\lambda}\left[1 - e^{-2\pi h/\lambda}\right]. \tag{19}$$

Here g is the gap, λ is the period length and h is the height of the blocks. B_r is the remanent field of the magnet material.

In order to built a damping wiggler with a given damping integral I_D the total volume of magnet material required is given by :

$$V_m = \frac{2hwI_D}{\frac{1}{2}B_w^2} = \left(\frac{0.492\lambda w I_D}{B_r^2}\right)e^{2\pi g/\lambda}. \tag{20}$$

Here I_D is the damping integral in T^2m. In the above equation the height of the magnets which is chosen equal to $\lambda/4$, w is the width of the magnets. The factor $1/2$ in the denominator accounts for the sinusoidal field distribution. Eq.(19) and Eq.20) are shown graphically in Fig.2. Choosing λ equal to $2\pi g$ minimizes Eq.(20) which in this case becomes:

$$V_{min} = 8.403\frac{wgI_D}{B_r^2}. \tag{21}$$

The corresponding optimum field is given by

$$B_w^{opt} = 0.865 \cdot B_r. \tag{22}$$

Table 4 gives an overview of input parameters and results for the two damping ring alternatives under investigation. Fig. 4 shows a cross section and flux line distribution of half a period of the upper half of the structure in the $X - Y$ plane. The electron beam axis at $Y = 0$ along the Z direction. Fig. 5 shows the field profile along the Z axis.

The amount of material required is inversely proportional to B_r^2. More demanding B_r values are therefore desired to reduce the overall length. The results in Table 4 were therefore calculated for two values of B_r. State-of-art NdFeB material is assumed with $B_r = 1.2$ T for the first alternative. Top quality material with $B_r = 1.35$ T is commercially available.

The pure permanent magnet design described above is widely used. Numerous wigglers based on this proposal have been built for synchrotron radiation sources and free electron lasers as well. A fixed gap device can be built in an open $C-$frame configuration in a mechanically simple and compact way. The pure permanent magnet structure is completely free of iron. So external fields can be superimposed. Therefore external

Table 1: Preliminary Design Parameters for the 1.0 T Pure Permanent Wiggler with Sinusoidal Field Distribution

Parameter		Unit	Dog-Bone DR	PETRA DR
Damping integral	I_D	T^2m	870	100
Magnetic gap	g	mm	25	25
Width of magnet	w	mm	50	50
Period length	λ	mm	157.1	157.1
Remanent field	B_r	T	1.2 / 1.35	1.2 / 1.35
Peak field	B_w	T	1.033 / 1.16	1.033 / 1.16
Wiggler length	L	m	1627 / 1289	187 / 148
Volume of material	V_m	m^3	6.4 / 5.04	0.735 / 0.58
Material per meter		kg/m	29.7	29.7

horizontal as well as vertical correctors can be used without disrupting the wiggler. For very long devices like those under investigation this might be very useful.

3.4 1.5 T Square Wiggler

The schematic layout of another square wiggler with a much higher magnetic field is shown in Fig.6. Fig.7 presents one fourth of the cross section perpendicular to the beam axis together with a flux line distribution. A much larger magnet cross section is chosen. The magnet material again works at the $(B \cdot H)_{max}$. Conically shaped pole pieces were selected which minimize leakage flux. In an analogous way to the 0.5 T wiggler a rectangular field distribution along the beam axis is produced. The peak field in this case is 1.5 T. Using Eq.(10) the maximum period length should not exceed 0.4 m. The increased peak field leads to a significantly reduced overall length. The total length of the wiggler section should be increased by a factor of $1/(1-g/\lambda)$ in order to account for the deviation from a

rectangular field distribution in the transition between positive and negative field sections. This results in a 7% correction for $\lambda = 400$ mm and $g = 25$ mm.

Preliminary design parameters of the 1.5 T wiggler are summarized in Table 5.

Table 5: Preliminary Design Parameters for the 1.5 T Square Wiggler

Parameter		Unit	Dog-Bone DR	PETRA DR
Damping integral	I_D	T^2m	870	100
Magnetic gap	g	mm	25	25
Width of magnet	w	mm	30.4	30.4
Height of magnet	h	mm	102	102
Period length	λ	mm	<400	<400
Peak field	B_0	T	1.5	1.5
Wiggler length	L	m	387	44.4
Volume of material	V_m	m^3	4.79	0.55
Material per meter		kg/m	93	93

3.5 2.0 T Square Wiggler

Fig.8 shows a cross section perpendicular to the beam axis through a square wiggler which results in a field amplitude of 2.0 T. The cross section of the pole is now rectangular and there is now room for an additional magnet on top. The geometry is very simple. Only rectangular soft iron plates, magnets and pole pieces are used. The period length of this device should not exceed 0.32 m in order not to violate the emittance growth condition given by Eq.(10). As in the previous examples the working point of the magnet material is close to $(B \cdot H)_{max}$. Table 6 gives a summary of the design parameters. It is seen that the total length is again reduced significantly as compared to the previous examples.

Table 6: Preliminary Design Parameters for the 2.0 T Square Wiggler

Parameter		Unit	Dog-Bone DR	PETRA DR
Damping integral	I_D	T^2m	870	100
Magnetic gap	g	mm	25	25
Width of magnet	w	mm	100/50	100/50
Height of magnet	h	mm	50/50	50/50
Period length	λ	mm	<320	<320
Wiggler length	L	m	218	25
Volume of material	V_m	m^3	5.44	0.625
Material per meter		kg/m	187.5	187.5

4 Discussion

In the preceding sections four different proposals have been discussed to build a damping wiggler. Table 7 briefly summarizes the following parameters of these options: total length of wiggler section, total required amount of magnetic material (NeFeB with remanent field of 1.2 T), and an estimate estimation of natural chromaticity contribution accordingly to Eq.(15).

One can see that chromaticity is certainly an issue for the "dog-bone" damping ring with 0.5 T and 1.0 T wigglers.

While the total amount of magnet material differs only by 10-15% the peak field level differs by a factor of four and consequently the lengths differ by a factor of 16 ranging from 25 to about 400 m for the PETRA damping ring version and from 218 to 3480 m for the Dog bone ring. Clearly the amount of magnet material is an important cost factor but not the only one. For an economical comparison other aspects also have to be considered like simplicity or complexity and mechanical design of the mechanical supports, magnetic forces, vacuum chamber design, absorbers for synchrotron radiation,

Table 7: Comparison of TESLA DR Wiggler Options

Parameter	Permanent Magnet Wigglers			
Max. Field	0.5 T	1.0 T	1.5 T	2.0 T
Wiggler length [m]:				
for 20-km DR	3480	1630	387	218
for 2.3-km DR	400	187	44	25
Required NeFeB [kg]:				
for 20-km DR	40,370	48,400	36,000	40,900
for 2.3-km DR	4,640	5,550	4,100	4,690
Chromaticity of wiggler section:				
for 20-km DR	-70	-33	-7.7	-4.4
for 2.3-km DR	-8.0	-3.7	-0.9	-0.5

etc. A C-type wiggler should be preferred if a vacuum system with an antechamber is used. Some access to the vacuum system has to be provided in any case in order provide sufficient pumping power. This also favors designs which allow some access to the beam region.

The size of the field filled volume is an important cost factor as was demonstrated by Eq.(17). It therefore should be chosen as small as possible. The available insertion space in the damping ring has also to be considered which has to be provided in a dispersion free part of the ring. Thus one might wish to limit the total length of the wiggler or to split it up in a number of subsections if this space is limited.

Finally, the field quality in magnets using iron poles does not strongly depend on the quality of PM material. This can be an important cost factor as well and should be taken into consideration.

References

[1] R.Brinkmann, *Proc. of IEEE PAC'95*, Dallas (1995),
see also DESY Internal Report M-95-08 (1995), pp.57-59.

[2] K.Flöttmann, DESY 93-161 (1993).

[3] J.Rossbach, *Nucl. Instr. Meth.*, A309, p.25 (1991).

[4] E.Colby et.al, *Proc. of IEEE PAC'95*, Dallas (1995).

[5] K.Flöttmann, J.Rossbach, *Proc. of EPAC'94*, London, vol.1, p.503 (1994),
see also DESY Internal Report 94-03-K (1994).

[6] J.Pflüger, *Proc. of "Source'94" Workshop*, Schwerin, Germany, p.76 (1994).

[7] J.P.Delahaye, J.P.Potier, *Proc. of EPAC'94*, London (1994),
and CERN/PS 94-15 LP (1994).

[8] D.G.Koshkarev, DESY Print TESLA 95-16 (1995).

[9] P.R.Zenkevich, DESY Print TESLA 95-15 (1995).

[10] V.D.Shiltsev, DESY Print TESLA 95-22 (1995).

[11] H.Wiedemann, Particle Accelerator Physics I, Springer-Verlag (1993).

[12] K.Halbach, *Journal de Physique*, C1, Supp.2, c1-211 (1983).

[13] K.Halbach, *Nucl. Instr. Meth.*, 187, p.109 (1982).

[14] A.Dubrovin, *The 2D-3D MERMAID Code*, INP Novosibirsk (1994).

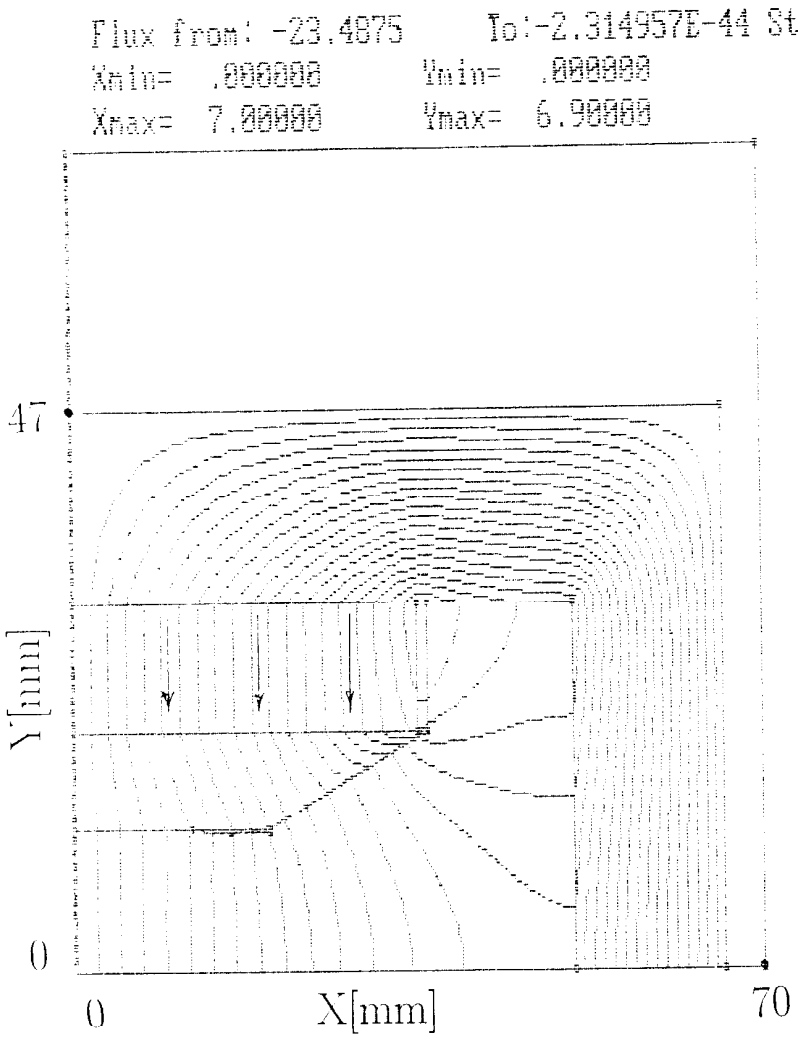

Fig.1: Magnetic field lines over the cross-section of the 0.5 T wiggler.

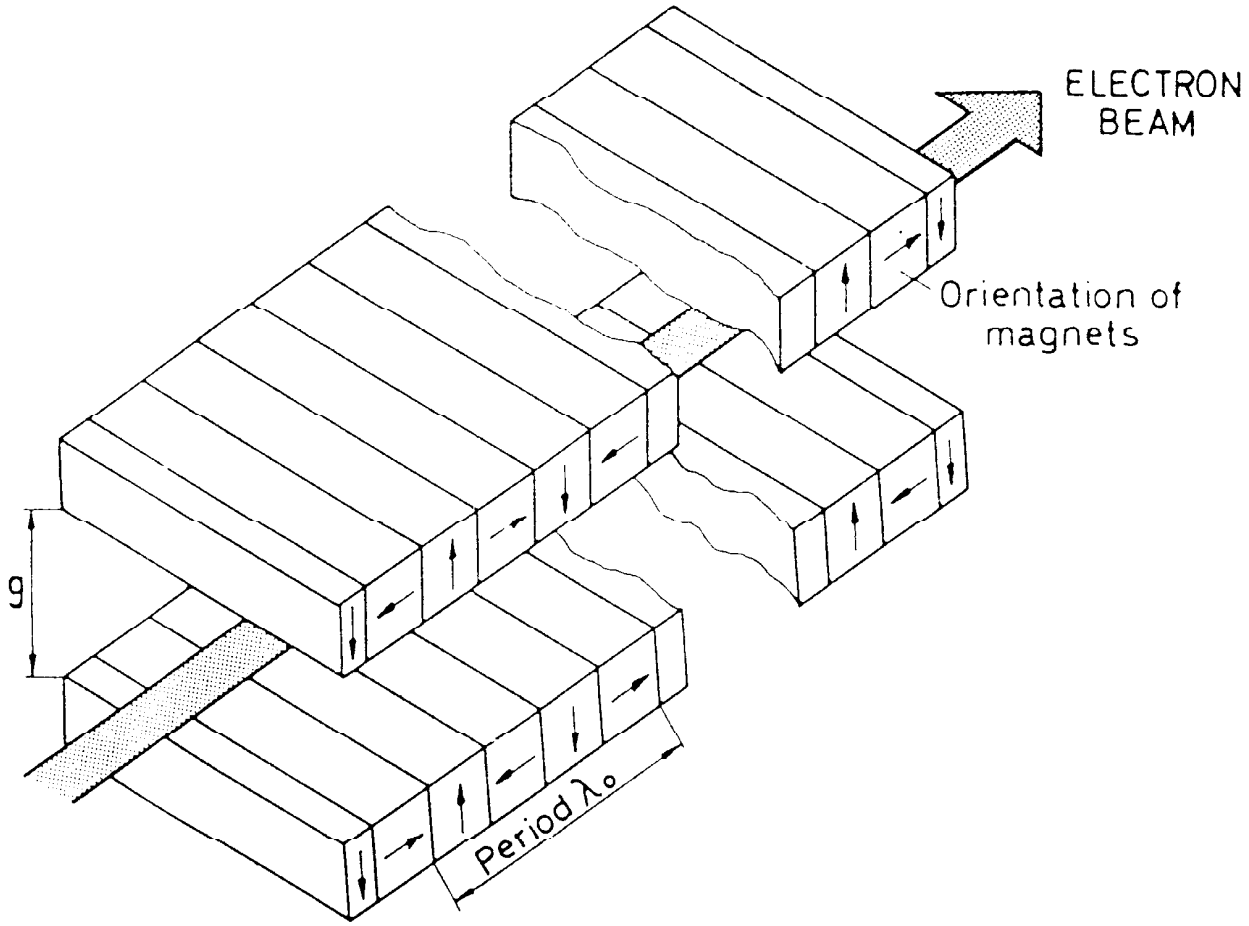

Fig.2: Layout of the 1 T wiggler.

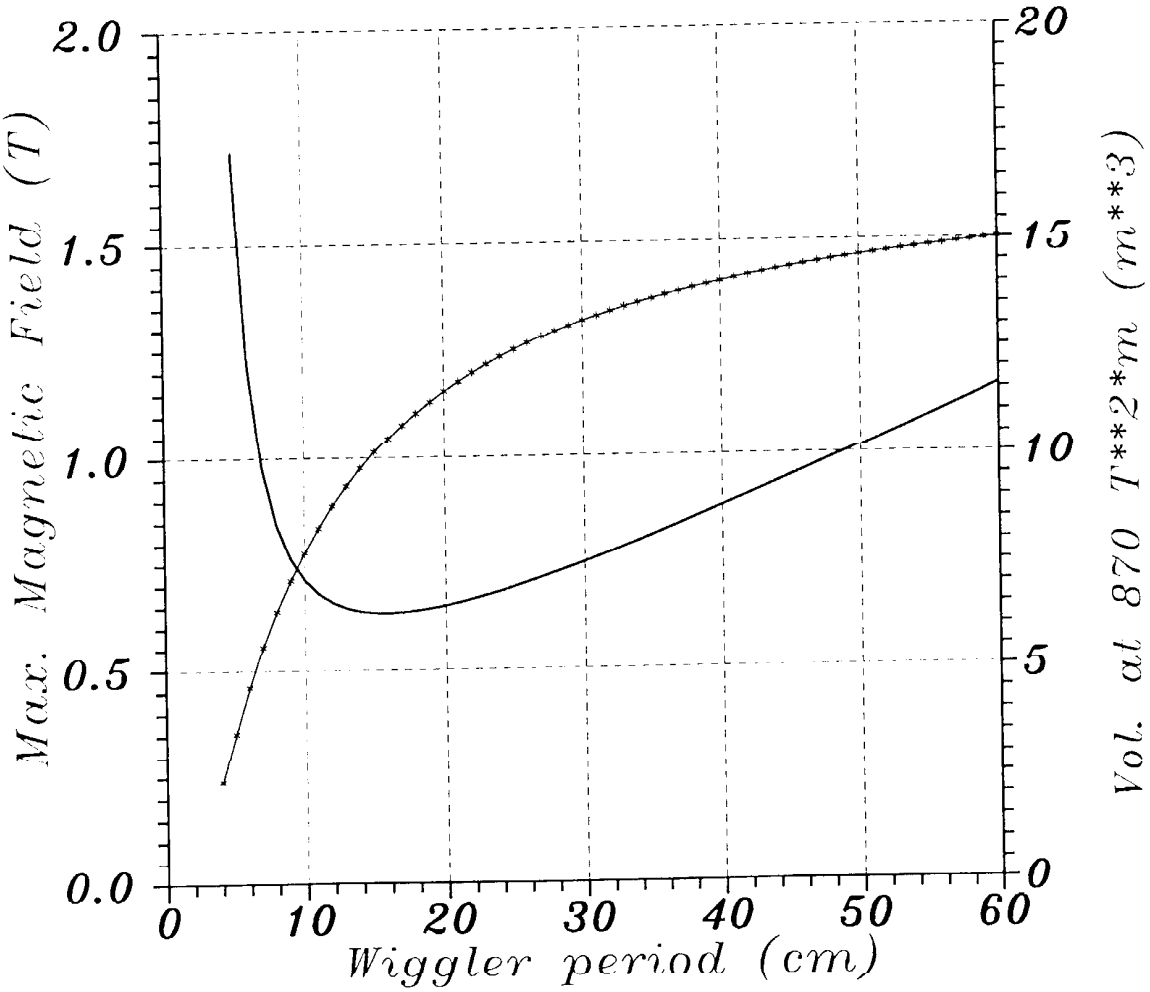

Fig.3: Maximum magnetic field (solid marked line) and required volume of magnetic material (solid line) vs. wiggler period for the Fig.2 design.

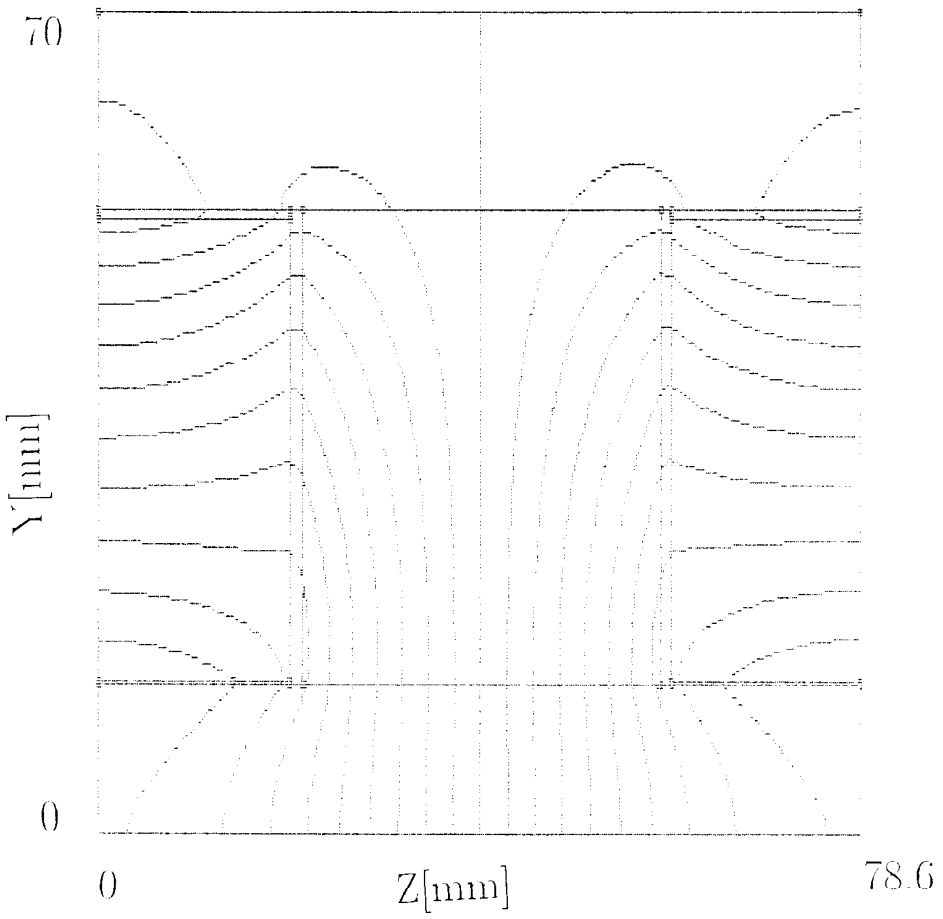

Fig.4: Magnetic field lines over the cross-section of the 1 T wiggler.

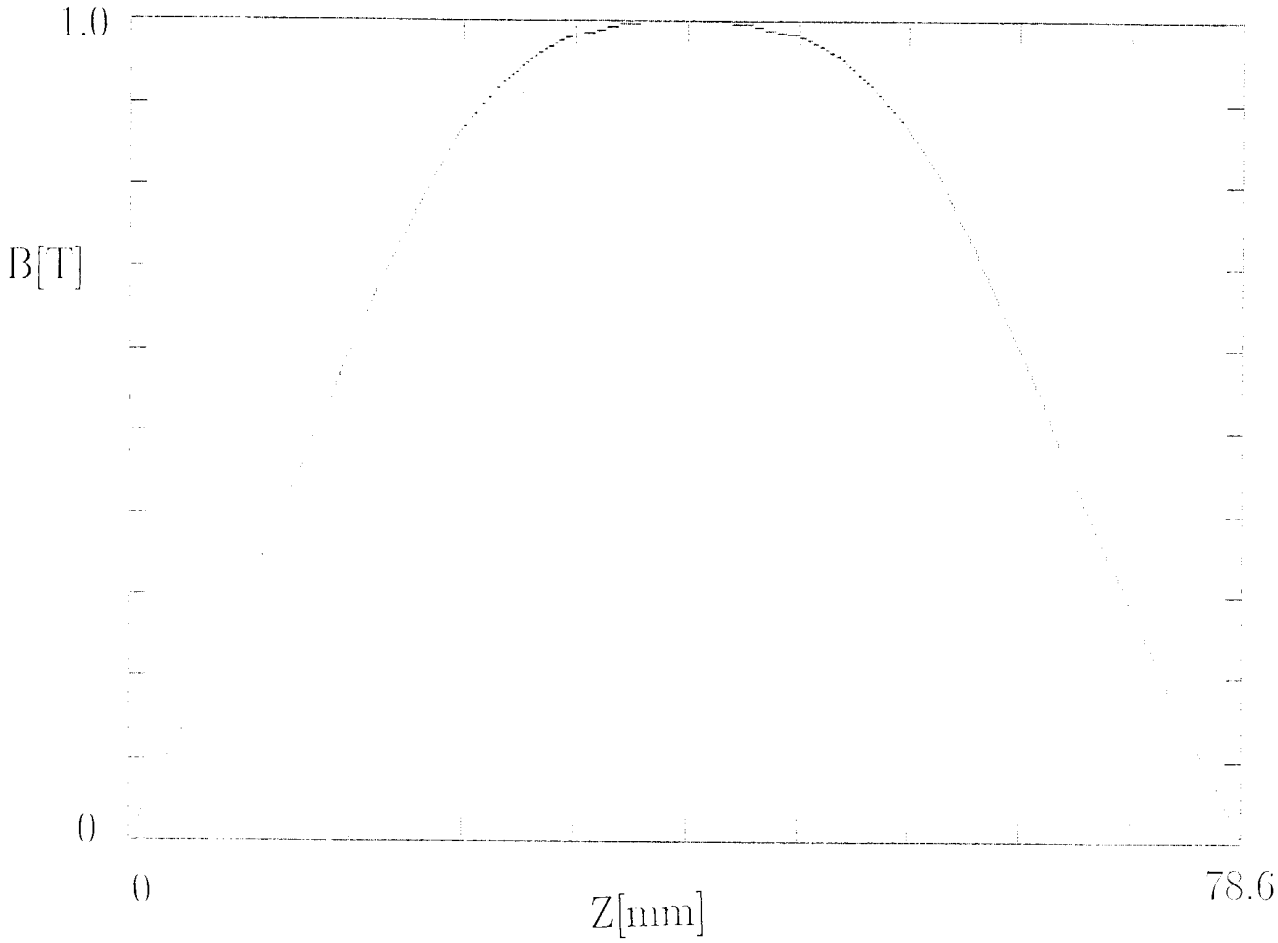

Fig.5: The vertical component of the magnetic field over the half period of the 1 T wiggler.

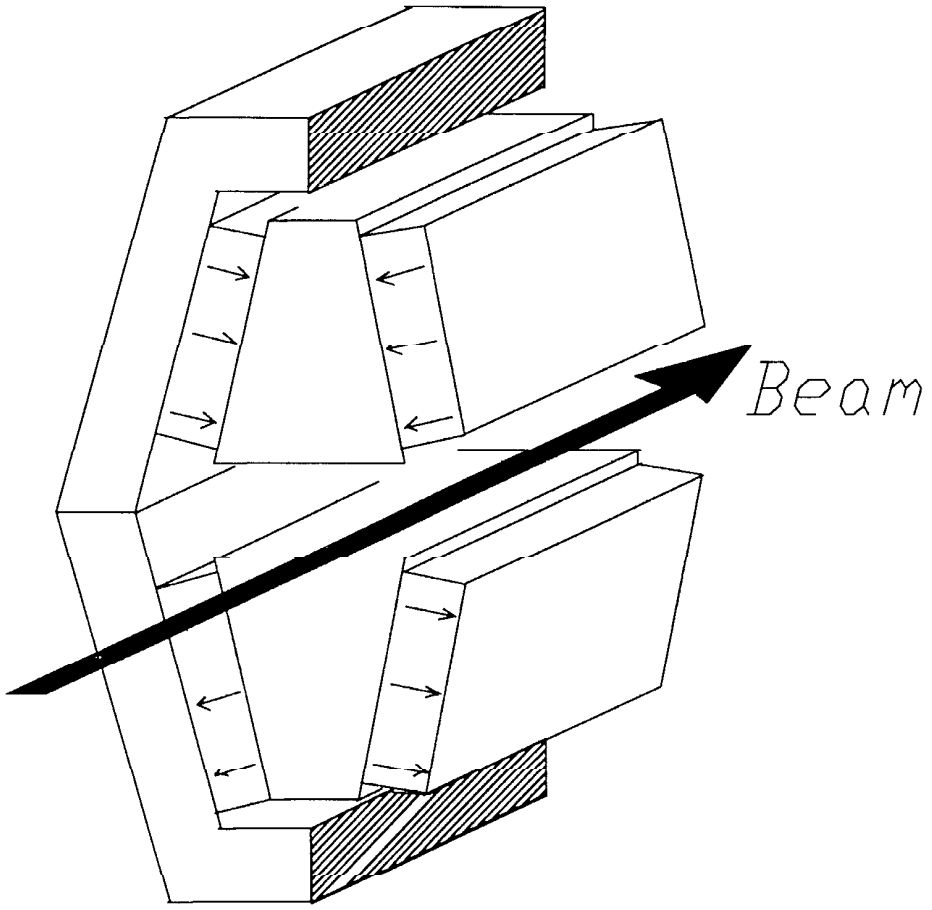

Fig.6: Layout of the 1.5 T wiggler.

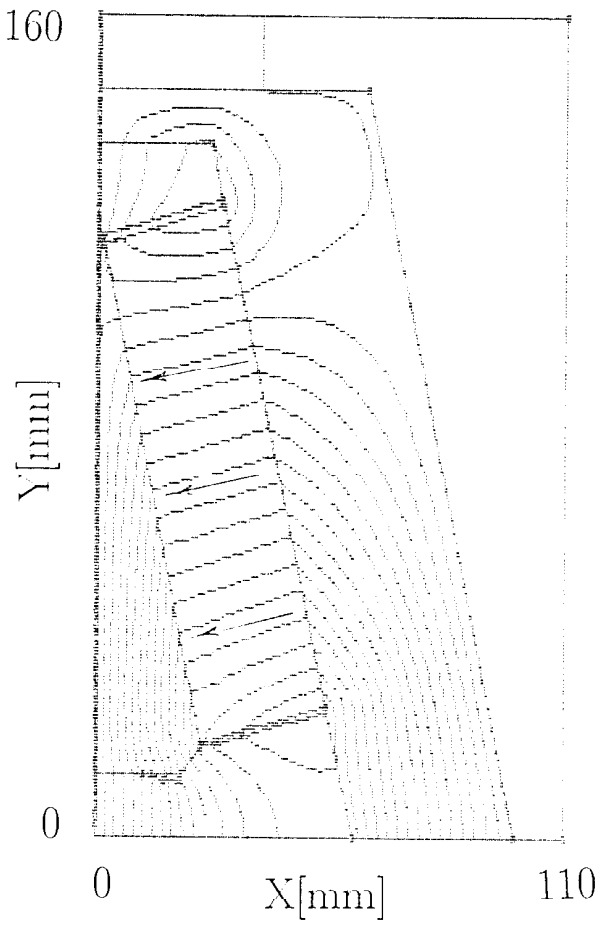

Fig.7: Magnetic field lines over the cross-section of the 1.5 T wiggler.

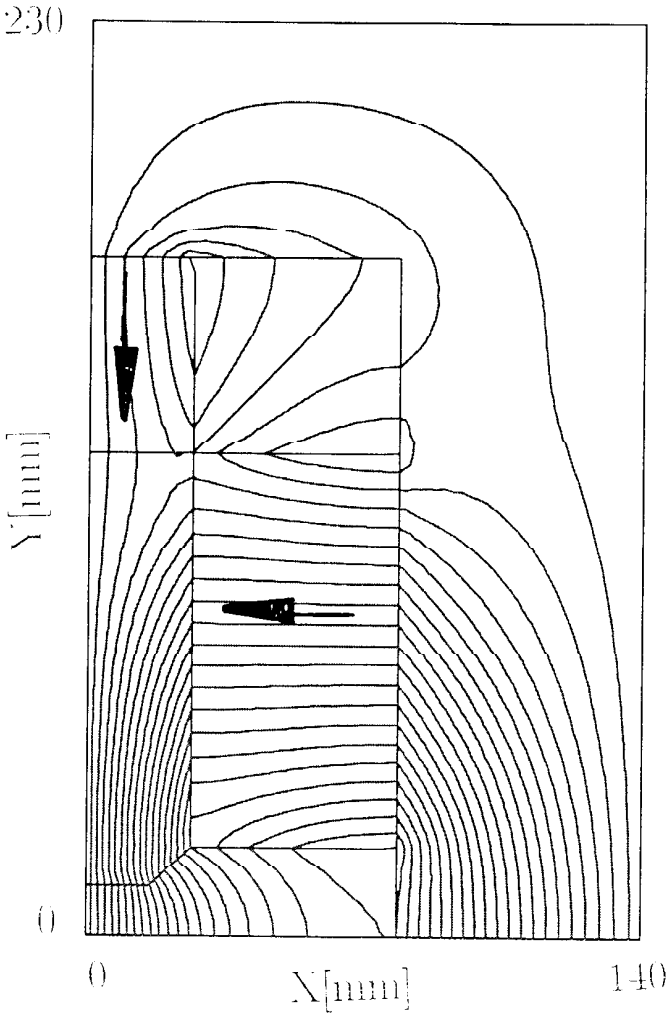

Fig.8: Magnetic field lines over the cross-section of the 2.0 T wiggler.